CHAPTER 1

Liquid Crystal Lasers

HIDEO TAKEZOE

Department of Organic and Polymeric Materials, Tokyo Institute of Technology, Tokyo, Japan

1.1 INTRODUCTION

Liquid crystals (LCs) have fluidity and a long-range orientational order. These properties enable us to use LCs as display materials. Another important property is a positional order. The periodicity is in the range not only of the molecular length periodicity like in smectic LCs but also of visible light wavelength. The latter generally arises from chirality, and in many cases results in helical structures. The most well-known example is cholesteric LCs (CLCs), in which the local structure is nematic and the director rotates to form a helical structure with the helical axis perpendicular to the director. The media that have periodic structures in the optical wavelength are called photonic crystals. Hence, we can call CLC a one-dimensional (1D) photonic crystal. Like an energy gap for electrons propagating in periodic crystal structures, a stop band emerges at the edges of the first Brillouin zone in CLCs. Within the stop band, light dampens and cannot propagate. When the light propagation is limited along any direction, we call it the photonic bandgap (PBG) [1, 2]. In this chapter, the stop band is called PBG in a broad sense.

The dispersion relation between angular frequency ω and wavenumber *k in vacuo* is given by $\omega = ck$, where c is the velocity of light (Figure 1.1a). In CLCs, the refractive index changes periodically, so the incoming light to the helix undergoes reflection if the light wavelength coincides with the optical pitch (structural pitch multiplied by an average refractive index), that is, Bragg reflection. Helical periodic structure makes the reflection very unique; that is, only a circularly polarized light (CPL) with the same handedness as the helix is reflected and another CPL with opposite handedness just passes through. This is called selective reflection. Such light propagation characteristics along the helical axis are rigorously solved, giving an analytical solution [3]. The dispersion relation thus obtained is shown in Figure 1.1b. Another unique feature compared with the other periodic structure is the sinusoidal

Liquid Crystals Beyond Displays: Chemistry, Physics, and Applications, Edited by Quan Li.

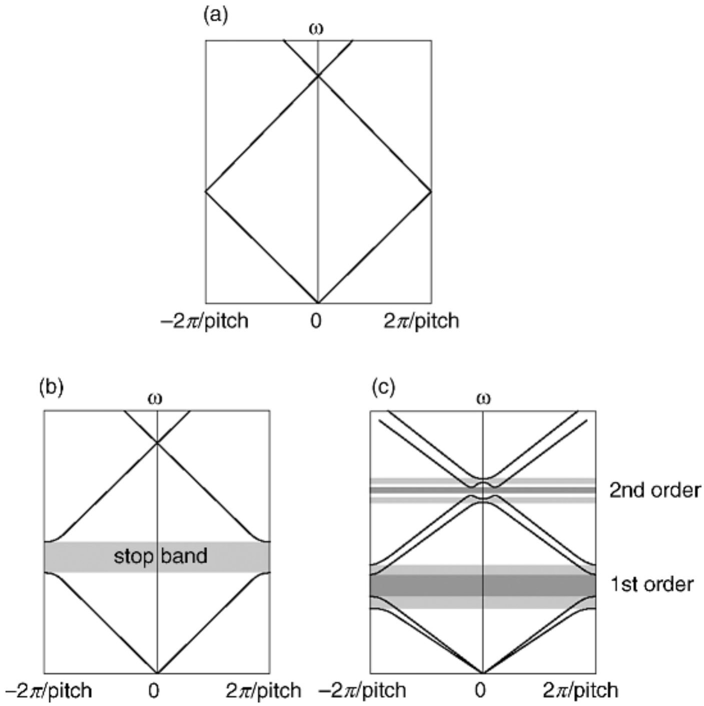

FIGURE 1.1 Dispersion relation (a) *in vacuo*, (b) in CLC at normal incidence, and (c) in CLC at oblique incidence. At oblique incidence, higher order reflection and total reflection regions are recognized.

change of the refractive index. Because of this, only the first-order Bragg reflection takes place (Figure 1.1b). For oblique incidence of light with respect to the helical axis, the periodic structure is no more than sinusoidal, so higher order reflections occur [4]. In addition, total reflection band(s) emerges, where light with any polarization states is reflected [5]. The dispersion relation (Figure 1.1c) calculated by the 4×4 matrix method [6] clearly reveals such behaviors. The emergence of higher order reflections and total reflection can be brought about by deforming the sinusoidal helical structure, for example, by applying an electric field. Such optical properties are similarly observable in other helical LC phases such as chiral smectic C* (SmC*) and twist grain boundary (TGB) phases.

Because of the selective reflection in visible wavelength regions, it is a natural question how the emission from dye molecules existing inside the helical structure is affected by the Bragg condition. Actually, Kogelnik and Shank [7] studied possible distributed feedback (DFB) lasers. Namely, lasing may occur if emitted light is confined in a DFB cavity made of CLC. The lifetime of the luminescence from dyes embedded in CLCs was also examined [8, 9]. The first observation of lasing from CLC was reported by Il'chishin et al. in 1980 [10]. They even showed the lasing wavelength tuning by temperature. However, it took almost two decades to be paid much attention from other groups until Kopp et al. [11] reported a CLC microlaser. For historical details, please refer to an article by Bartolino and Blinov [12].

Let us consider efficient lasing conditions. In an isotropic medium, the rate R of photon emitted from an excited molecule is described by Fermi's golden rule:

$$R_{\text{iso}} \sim M_{\text{iso}} |E \cdot \mu|^2 \tag{1.1}$$

where M_{iso} is the density of state (DOS), μ is the transition dipole moment, and E is the electric field. In isotropic media, M is independent of the polarization and the radiation direction. In anisotropic media, the emission depends on the orientation of transition dipole moment μ with respect to the polarization of light, that is, E. When emission occurs from the excited CLC molecules, light propagates as one of the two eigenmodes E_1 and E_2. Then, emission rate for eigenmode E_i (R_i) is described as

$$R_i \sim M_i |E_i \cdot \mu|^2 \tag{1.2}$$

where M_i is the DOS associated with the eigenmode E_i. The fluorescent molecules embedded in CLCs have a certain degree of the nematic order, resulting in an anisotropic orientation distribution of the transition dipole moment. Hence to have large R_i, it is profitable that μ is parallel to the polarization of the eigenmode E_i. Now the other factor to have large R_i is DOS M, which is defined as

$$M = \left| \frac{\mathrm{d}}{\mathrm{d}\omega} \mathrm{Re}(k) \right| \tag{1.3}$$

Figure 1.2 shows a simulated transmittance spectrum and DOS (M). DOS shows maxima at the PBG edges where group velocity approaches to zero.

1.2 TYPES OF LASERS

There are several types of CLC microlasers. DFB lasers and defect mode lasers are the most popular ones, which will be described later. For more detail on these modes, please refer to a review by Kopp et al. [13]. In this chapter, we do not include random lasing and lasing from artificial structures such as grating.

1.2.1 DFB CLC Lasers

When light propagates in periodic media with the same periodicity as the light wavelength, the light suffers reflection due to the PBG. Hence, if CLC is doped with dyes, emitted light within the PBG is confined and amplified in CLC, and finally lasing results. This type of cavity without using mirrors is called DFB cavity. Lasers using DFB cavities are called DFB lasers. The DFB cavity is widely

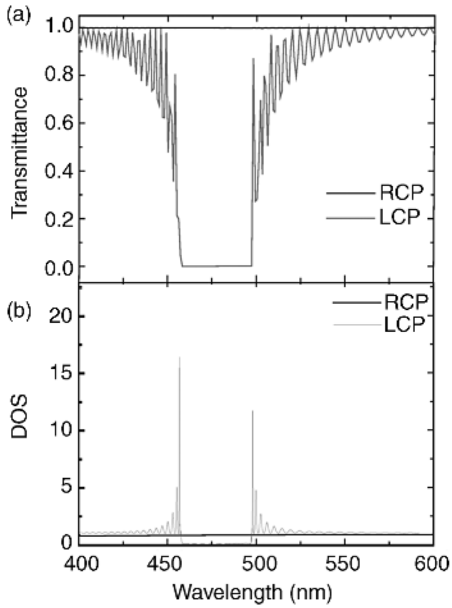

FIGURE 1.2 Simulated transmittance spectrum and DOS spectrum for R- and L-CPL to left-handed CLC at normal incidence [79].

used in semiconductor lasers, in which active materials are on substrates with periodic refractive index changes. Since CLCs themselves spontaneously form DFB cavity, this is the simplest CLC microlaser structure. Namely, instead of fabricating layer-by-layer structures consisting of high and low refractive indices as in semiconductor lasers, the refractive indices in CLC change due to the helical structure of the dielectric ellipsoid. This is a great advantage of CLC microlasers compared with semiconductor lasers, in which the fabrication of microstructure is necessary.

Dowling et al. [14] predicted that DFB lasing occurs at the edge of PBG for 1D periodic structures with sufficiently large refractive index modulation. They demonstrated that the photon group velocity approaches zero near the band edge of a 1D photonic bandgap structure. This effect implies an exceedingly long optical path length in this structure, and the photon dwell time for incident waves at the band edge is significantly increased. M in Eq. (1.3) is the absolute inverse slope of the dispersion relation or reciprocal form of group velocity. Since the emission rate R is proportional to DOS, the emission rate reaches maximum when group velocity falls to almost zero, which is realized at the edges of PBG, as shown in Figure 1.2b. Thus, low-threshold and mirrorless CLC laser is realized at the edges of PBG, where DOS gives maxima.

Experimentally, two major structures are possible in CLC microlasers; the helical structure is perpendicular or parallel to substrates. The former is rather easy to be fabricated by using substrate surfaces treated with planar alignment agents.

Homeotropic alignment surfaces give orientation with helical axis parallel to the surface. However, the orientation of helical axis to a particular direction is not easy.

Optical eigenmodes at the edges of PBG are linearly polarized in CLCs; they are perpendicular and parallel to the local director at the higher and lower energy edges, respectively. According to Eq. (1.2), R_i is larger at the lower energy edge, so lasing preferably occurs at the lower energy edge [15]. A simple theoretical description of the spontaneous emission as a function of wavelength in terms of the order parameter S for the transition dipole moment of the dye in the CLCs is as follows [16]:

$$\left\langle |E \cdot \mu|^2 \right\rangle = \frac{2}{3} \frac{\rho_i^2 - \frac{1}{2}}{\rho_i^2 + 1} S_{\text{dye}} + \frac{1}{3} \tag{1.4}$$

Here, ρ_i is the ellipticity of polarization state. Figure 1.3a shows calculated $\left\langle |E \cdot \mu|^2 \right\rangle$ in CLCs with the local director of the order parameter $S = 1.0$, 0.5, 0.2, 0, and -0.5 for the incidence of left circularly polarized light as a function of wavelength. Near the edges of photonic bandgap, the variation in $\left\langle |E \cdot \mu|^2 \right\rangle$ occurs sharply, because the polarization states of the eigenmode with the same handedness as the CLC's

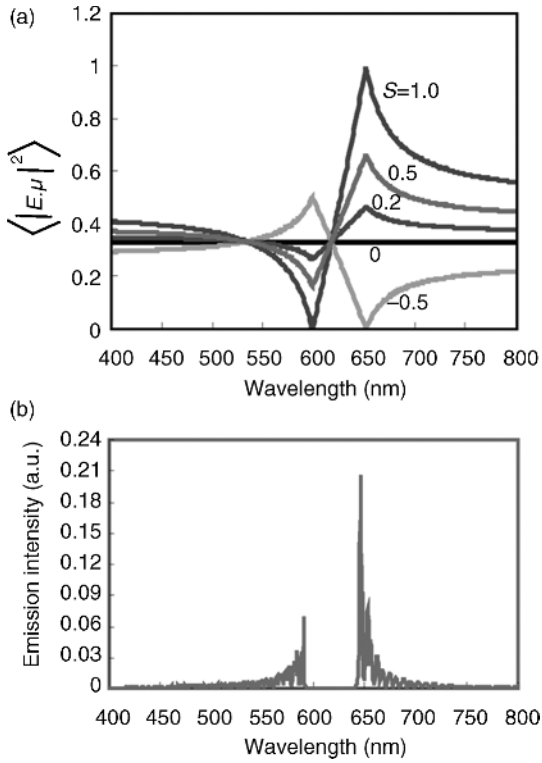

FIGURE 1.3 (a) Calculated $\left\langle |E \cdot \mu|^2 \right\rangle$ against wavelength for several S values. (b) Emission rate as a function of wavelength for $S = 0.5$.

structure is linearly polarized along the local director of the CLC. Particularly, at the low-energy edge of photonic bandgap, the value of $\left\langle |E \cdot \mu|^2 \right\rangle$ is high because the polarization direction is parallel to the local director of the CLC. However, at the high-energy edge of PBG, the $\left\langle |E \cdot \mu|^2 \right\rangle$ value is low because the polarization direction is perpendicular to the local director of the CLC. Then, the emission rate R_i (Eq. (1.2)) takes the highest value at the low-energy edge, as shown in Figure 1.3b.

1.2.2 Defect Mode Lasing

By doping semiconductors with donor or acceptor, donor or acceptor level is introduced within energy gaps. Similarly, addition or removal of extra dielectric material locally inside the photonic crystal produces donor or acceptor level [17]. DOS at such defect levels is much higher than that at PBG edges, so defect mode lasing is very important to realize low-threshold lasing. Many types of defect mode have been studied in 1D [13, 14, 18], 2D [19], and 3D [20, 21] photonic structures. These can be produced by removing or adding material or by altering the refractive index of one or a number of elements in 1D, 2D, and 3D PCs. Introducing a quarter-wavelength space in the middle of a layered 1D sample produces a defect in the middle of PBG. Such a defect is widely used to produce high-Q laser cavities [13].

Five kinds of configurations are suggested to generate a defect mode in CLCs (Figure 1.4): (1) the creation of a phase jump without any spacing layer in CLCs [22–24] and in smectic LCs [25], (2) the introduction of an isotropic spacing layer in the middle of the CLCs [26, 27], (3) the introduction of an anisotropic spacing layer in the middle of the CLCs [28, 29], (4) combination of (1) and (2) [30], and (5) the local deformation of the helix in the middle of the CLC layer [31].

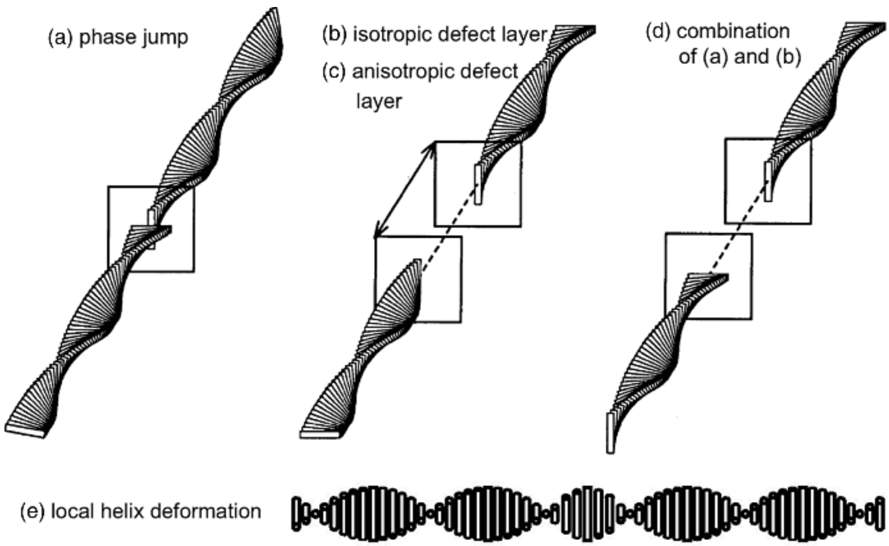

FIGURE 1.4 Five kinds of defect structures in CLCs.

The defect mode 1, that is, a chiral twist defect, can be created by rotating one part of the CLC [22, 23], as shown in Figure 1.4a. Changing the chiral twist angle from 0° to 180° tunes the defect wavelength from high- to low-wavelength PBG edge. By twisting one part of the CLC by 90°, a defect mode can be generated at the center of PBG due to the phase shift $\pi/2$ of electromagnetic wave inside the photonic bandgap. The defect mode 2 can be produced in a CLC structure by introducing isotropic layer between two CLC layers in order to destroy the helical periodicity of CLCs, as shown in Figure 1.4b [26]. For the thickness of the isotropic defect layer that generates the phase shift $\pi/2$, a defect mode can be generated at the center of PBG. This condition is expressed as

$$d = (2i + 1)\frac{\lambda}{4 \cdot n} \tag{1.5}$$

where d is the thickness of a defect layer, i is an integer, λ is the wavelength of the defect mode, and n is the refractive index of the defect layer.

Let us show one example of defect mode lasing of type 2 [27]. Figure 1.5 shows the simulation of transmittance and DOS in a CLC laser with a thin isotropic layer (0.54 μm thick poly(vinyl alcohol) (PVA) film) as an isotropic defect layer. A sharp defect level is observed, where highest DOS is obtained. Lasing was observed at

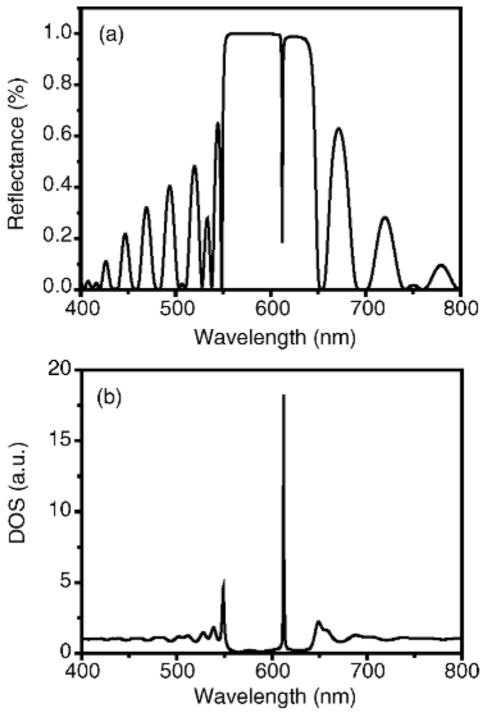

FIGURE 1.5 (a) Simulated transmittance spectrum and (b) DOS spectrum for CLC with an inserted isotropic defect layer [27].

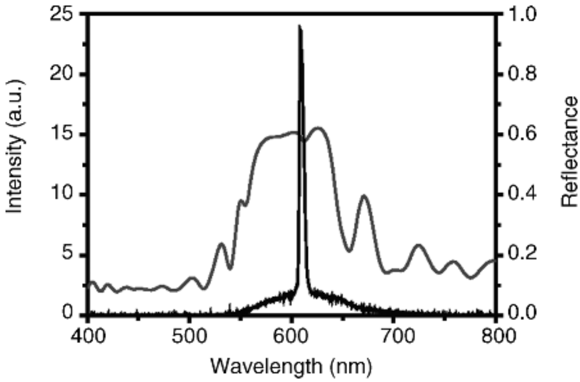

FIGURE 1.6 Lasing spectrum at the defect state together with a transmittance spectrum [27].

the defect wavelength, as shown in Figure 1.6. Since the device is composed of polymer CLC and PVA, one can peal out the film from the substrate as a freestanding film of 5.5 μm thickness.

1.3 LOWERING THRESHOLD

One of the ultimate goals of CLC microlasers is continuous wave (cw) lasing. For this purpose, the lasing threshold must be essentially zero. Many efforts have been made from various points of view. These efforts are classified into three groups: (1) improved cavity structures, (2) improved excitation conditions, and (3) improved materials. For (1), (1a) utilizing a single output window and (1b) utilizing defect mode were examined. For (2), (2a) excitation at the PBG edge by CPL and (2b) excitation at a higher energy (shorter wavelength) side of an absorption band were used. For (3), (3a) utilizing highly ordered dyes, (3b) utilizing CLCs with higher anisotropy of refractive indices, (3c) utilizing Förster energy transfer, and (3d) developing new dyes were examined.

1.3.1 Lowering Threshold by Improved Cavity Structures

Amemiya et al. [32] introduced polymeric CLC (PCLC) reflection layers for excitation light (PCLC pump substrate) as well as for outcoupled light (PCLC laser substrate), as shown in Figure 1.7, and succeeded in reducing the threshold by a factor of 2 (Figure 1.8). Matsuhisa et al. [33] used multiple inorganic layers for the similar purpose and obtained lower lasing threshold than the normal cell. It is known that the defect mode has an advantage to have higher DOS, as shown in Figure 1.5. Actually, Schmidtke et al. [23] and Ozaki et al. [24] demonstrated low-threshold defect mode lasing by using a phase jump in CLCs. As shown in Figure 1.9, the threshold in defect mode lasing is more than one order of magnitude smaller than that in the PBG edge lasing. The other group also obtained the similar results [27].

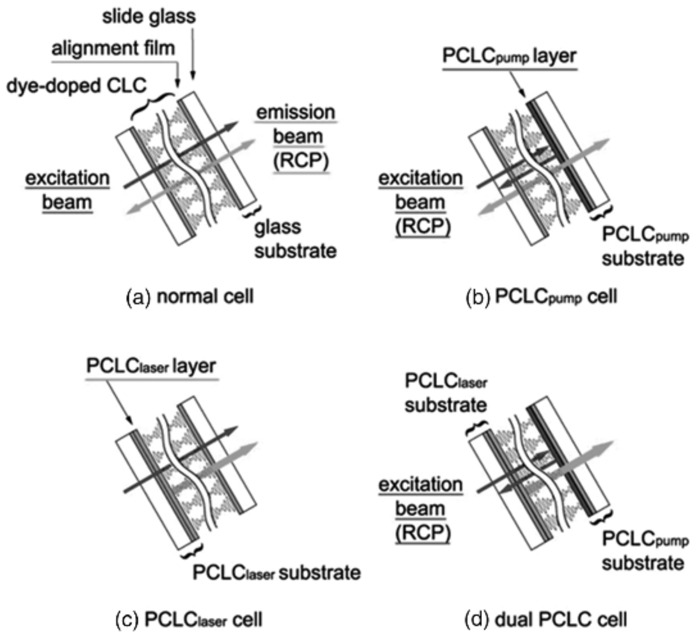

FIGURE 1.7 Some kinds of cell structures: (a) simple CLC cell, (b) CLC cell with PCLC layer for reflecting excitation light, (c) CLC cell with PCLC layer for reflecting emitted light, and (d) CLC with PCLC layers for reflecting both excitation and emitted light [32].

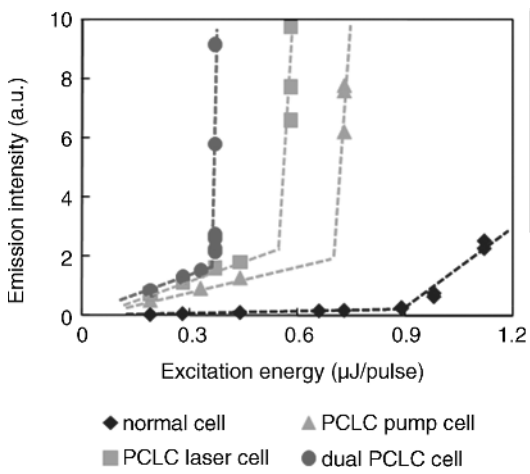

FIGURE 1.8 Threshold behavior for four cell geometries illustrated in Figure 1.7.

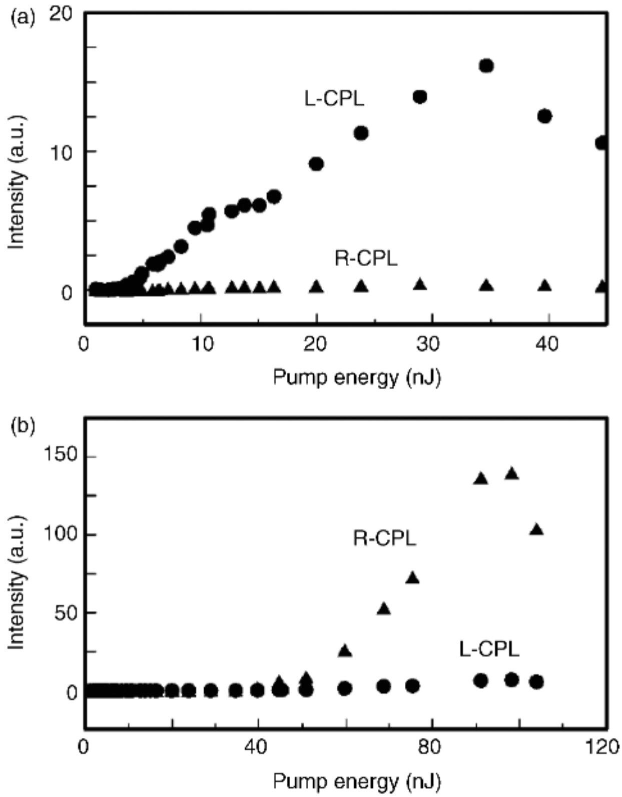

FIGURE 1.9 Threshold behavior for (a) defect and (b) DFB modes [23].

1.3.2 Lowering Threshold by Improved Excitation Conditions

If the dwell time at the excitation wavelength is long, efficient use of excitation energy can be achieved [34]. This condition can be realized by the excitation using CPL of the same handedness as the CLC helix at the first minimum of the subsidiary oscillation in the higher energy side of the reflection band [35]. Figure 1.10 shows the result in a dye-doped right-handed CLC (R-CLC). At 532 nm, R-CPL excitation gives lower threshold than left-handed CPL (L-CPL) excitation. Surprisingly, the threshold also depends on the excitation wavelength. Although the reason is not clear, it was confirmed using three different dyes that excitation at higher energy side of absorption bands gives lower threshold [36].

1.3.3 Lowering Threshold by Improved Materials

The efforts for lowering threshold have been made also from materials sides. As host materials, CLCs with higher anisotropy of the refractive index are more profitable. This is because PBG width is proportional to the anisotropy, and wider PBG gives

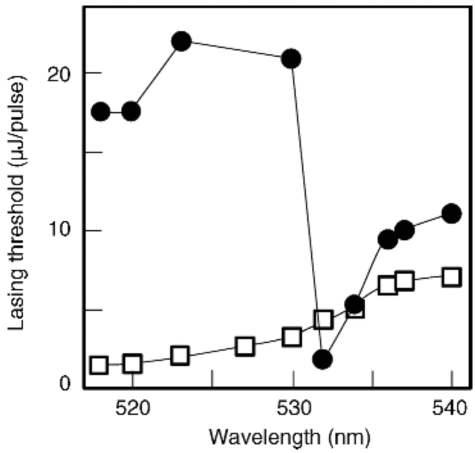

FIGURE 1.10 Lasing threshold as a function of wavelength for R- and L-CPL incidence to right-handed CLC cell [35].

higher DOS at the edges. This was experimentally confirmed by using three CLC hosts with different anisotropies of the refractive index [37]. The development of dyes is also important; first, highly ordered dyes are preferable because of Eq. (1.2) [15, 38]. As shown in Figure 1.3, the higher the order parameter S of dyes, the higher the DOS at the lower energy edge of PBG. In this sense, poly(phenylene vinylene) with triptycene groups is interesting, since S increases with increasing dye concentration. It is also known that the use of appropriate energy transfer between dye molecules (Förster couples) is possible to reduce the threshold. Reabsorption of the emitted light is a serious problem because it is one of the losses for lasing. In this sense, the use of energy transfer is one of the solutions to avoid reabsorption [39, 40]. Figure 1.11 shows the absorption and emission spectra of three dyes and threshold behaviors in the mixture systems containing two of these dyes. In both cases, the threshold is lower when the excitation through energy transfer is used compared with that by direct excitation.

So far, most of researchers have used commercially available dyes. Uchimura et al. [41] systematically synthesized pyrene and anthracene derivatives and evaluated the lasing characteristics. They found that one of the pyrene derivatives (Figure 1.12) shows a threshold as low as 1/20 of that in a commercial dye DCM. It was found that the threshold becomes lower with increasing luminous efficiency and radiative decay rate, as shown in Figure 1.12. We also need to systematically study the stability of dyes against light excitation. In this respect, it is important to have dyes showing low lasing threshold to minimize damage as well.

Recently, Wei et al. [42] used oligofluorene as a red-emitting dye and showed the superiority compared with a commercial DCM. Moreover, glassy CLC containing this dye is temporally stable compared with fluid CLC, lasing emission from which decays with time. Glassy state is important to realize robust sustainable lasing devices.

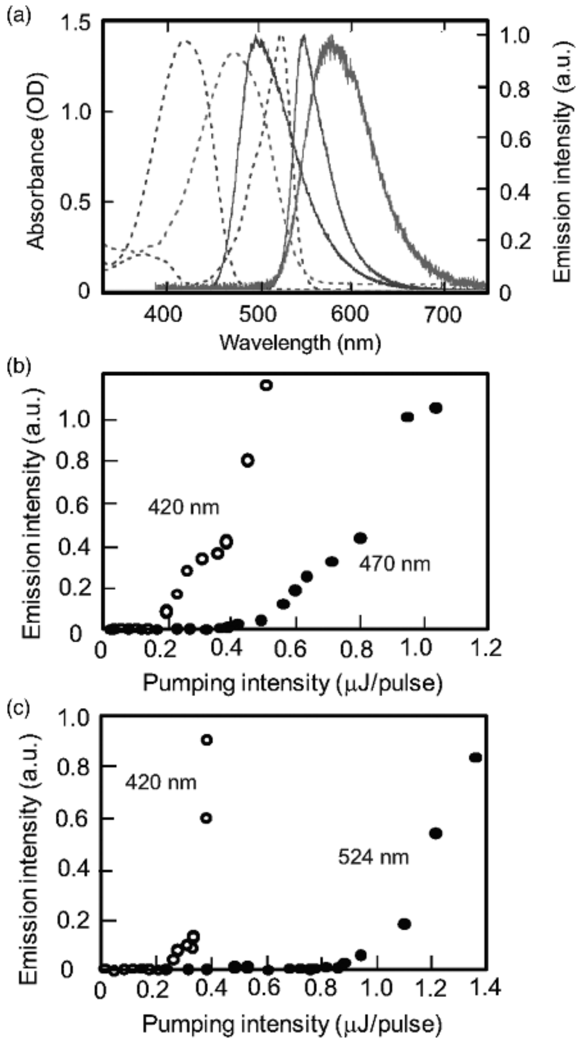

FIGURE 1.11 (a) Absorption (dotted curves) and emission (solid curves) spectra of dyes used as two kinds of Förster couples. Coumarin (C153), DCM, and pyrromethene (PM580) with increasing wavelength of the absorption peaks. Lasing threshold for direct and indirect (energy transfer) excitations to CLC cell with (b) C153 and DCM and (c) C153 and PM580 [39].

1.4 TUNABILITY

Wavelength tunability is one of the most attractive features in CLC lasers. Since the DFB lasing occurs at either or both of the edges of PBG, most of the cases at the lower energy edge, tuning of lasing wavelength is possible by tuning the helical pitch. There are many factors influencing the helical pitch: (1) temperature, (2) electric field, and (3) light irradiation. For polymer samples, (4) mechanical strain can also be used.

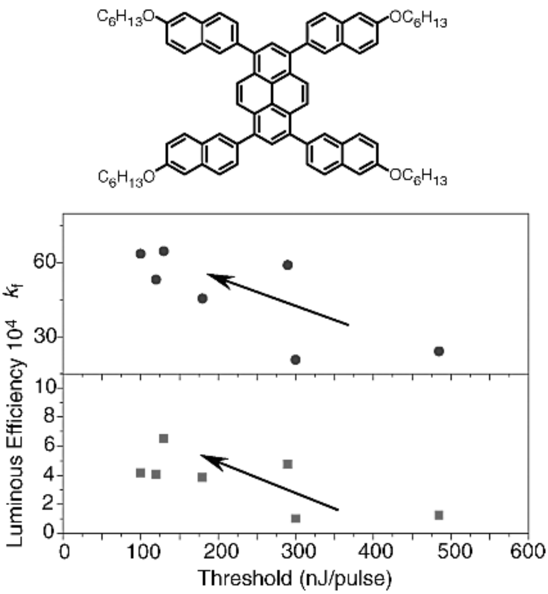

FIGURE 1.12 Relationship between luminous efficiency, radiative decay rate, and lasing threshold. The chemical structure of a pyrene derivative is also shown at the top.

In addition, (5) spatial tuning is a practical method for wavelength tuning, and (6) multiple lasing is also interesting.

1.4.1 Thermal Tuning

It is well known that the helical pitch in CLCs sensitively varies with temperature. Hence, thermal tuning was achieved by many scientists [38, 43] even from the very beginning [10]. Quite wide range of tuning like 30–60 nm is possible using single dye containing CLCs. However, the tuning is not really continuous because of the surface pinning of molecules. For the alignment with the helical axis perpendicular to the surface, surfaces have to be homogeneously treated. Since the molecular orientation at surfaces is fixed, number of pitch is quantized to be multiple numbers of half a pitch. The neighboring band edge wavelength λ and $\lambda + \Delta\lambda$ is given by

$$\frac{nd}{\lambda} - \frac{nd}{\lambda + \Delta\lambda} = \frac{1}{2}$$

where n is an average refractive index. Figure 1.13 shows the result using $d = 9\,\mu\text{m}$, $n = 1.66$, and $\lambda = 600\,\text{nm}$; $\Delta\lambda$ is 12.3 nm [43]. The discreteness can be reduced by using thick cells, but essential discreteness remains. To achieve real continuous tenability, devices with helical axis parallel to the surface were examined [44, 45]. Principally, thermal tuning in SmC* cavity must be continuous [46].

A different method for continuous wavelength tuning was examined by Morris et al. [47]. They used two different chiral dopants that exhibit opposing dependences

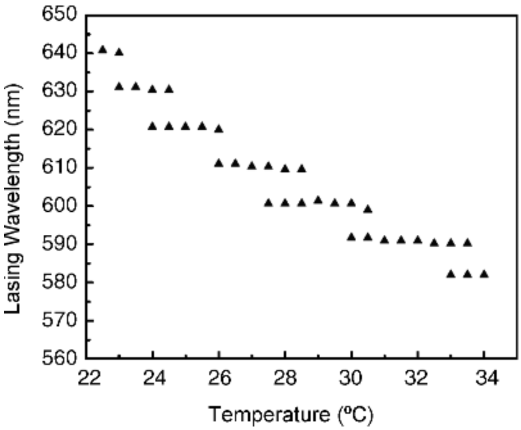

FIGURE 1.13 Temperature dependence of lasing wavelength in a CLC DFB laser [43].

of the natural pitch on temperature. Tuning over 15 nm was achieved using a 10 μm thick cell. However, the reason of the tunability in a cell, where the molecules at both surfaces are fixed, is not clear. Moreover, the cell quality might not be good judging from the wide lasing emission peak (~2 nm). Thermal tuning is also possible by using temperature-dependent chiral dopant solubility; that is, solubility of chiral dopant increases with increasing temperature, resulting in shorter pitch. Figure 1.14 shows the result [48]. Tuning over 60 nm was achieved.

1.4.2 Electric Field Tuning

It is also well known that helical pitch can be tuned by applying an electric field and is finally unwound under sufficient field strength. However, again surface pinning effect

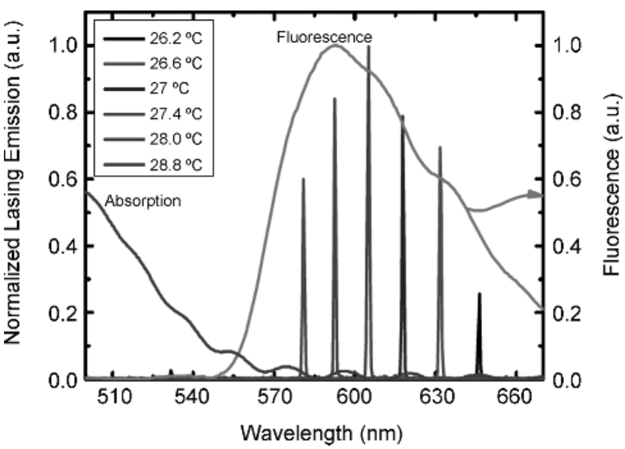

FIGURE 1.14 Lasing wavelength tuning as a function of temperature using temperature-dependent solubility of chiral dopant [48].

prevents the tuning of the helical pitch in cells with the helical axis perpendicular to substrates. Yoshida et al. [44] prepared wedge cells with the helical axis parallel to substrates and examined the tunability of lasing wavelength by applying an electric field. The field strength linearly depends on the position. Using such cells, position-dependent lasing wavelength variation over 100 nm was obtained. Electrotunable liquid crystal lasers are also possible using SmC* cells, since the surface pinning effect is negligible [46, 49].

Electrotunability of the lasing wavelength of the defect mode was also demonstrated using a layer of nematic liquid crystal (NLC) inserted into dielectric multilayers [18] and CLC layers [50]. This is based on the fact that the wavelength of defect modes continuously changes with the refractive index of the defect layer [26]. By applying an electric field, LC molecules change the orientation, resulting in effective refractive index, as shown in Figure 1.15a. Figure 1.15b is one of the results of electrotuning using defect mode lasing [51].

Another type of electrotuning was also demonstrated by Lin et al. [52]. They used CLC with negative dielectric anisotropy. By applying dc fields along the helical axis, the selective reflection band shifts toward shorter wavelength side. By applying an electric field of 150 V, lasing emission shifted by 15 nm. The field-dependent helical pitch was attributed to electrohydrodynamical effect. Similar but different

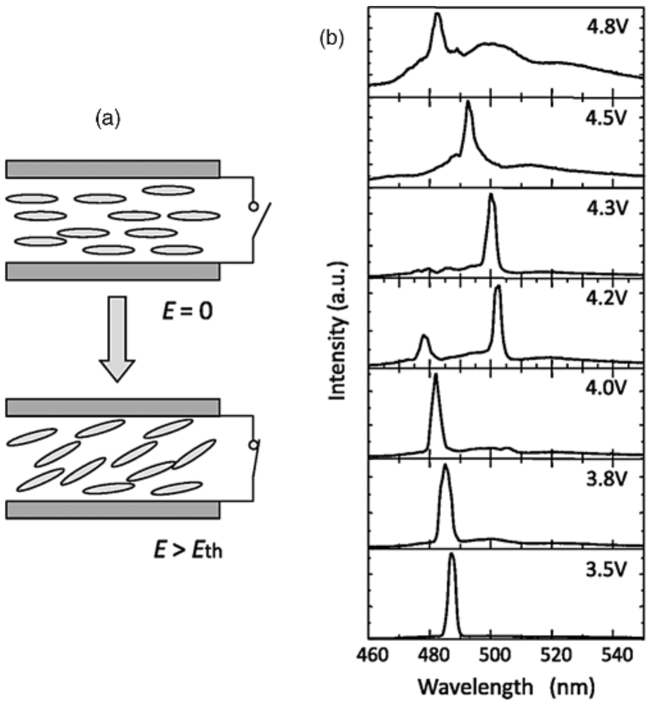

FIGURE 1.15 (a) Orientational change by applying an electric field. (b) Electric field-dependent lasing wavelength tuning of a defect mode using an anisotropic defect layer [79].

observation was made by Park et al. [53]. The sample used was NLCs embedded in helical polymer networks consisting of photopolymerizable CLC. With increasing electric field, transmittance spectra and color viewed from the substrate surface normal were blue shifted. The lasing emission was observed. However, the lasing peak does not show any wavelength shift but just becomes weak. In the absence of a field, lasing occurs toward the normal direction parallel to the helical axis. Surprisingly, however, under the field application, lasing emission is generated to any angle up to at least 70° with almost the same intensity as that in the normal direction. This phenomenon was interpreted as a spatial undulation of helical axis by Helfrich effect [54].

1.4.3 Phototuning

Several methods have been employed for wavelength tuning by light irradiation. Chanishvili et al. [55] prepared dye-doped CLCs. The photoexcitation of samples allows laser emission at about 400 nm. Phototransformation is induced by ultraviolet (UV) light irradiation in the structure of chiral molecules, leading to the change in the helical pitch (selective reflection peak) from 370 to 410 nm after 15 min irradiation. Since this process is irreversible, one or some compositions of chiral molecule mixture (Merck, ZLI-811) seem to be decomposed. In this sense, this is not real tunability.

A more practical method was proposed by Furumi et al. [56]. They used cholesteryl iodine, cholesteryl nonanoate, and cholesteryl oleyl carbonate as a host. UV irradiation at 254 nm resulted in continuous changes in the helical pitch from 550 to 720 nm depending on UV exposure energy. This phenomenon was attributed to photolysis reaction of the cholesteryl iodide. Lasing experiment using dye-doped samples reveals phototuning of laser wavelength over a 100 nm wavelength range.

Azomolecules are commonly used for phototuning of physical parameters. Lin et al. [57] used a chiral molecule with an azo linkage. Upon the irradiation of UV (350 nm) light for up to 20 min, selective reflection band becomes short over 100 nm. After 20 min UV irradiation, the photoisomerization from *trans* to *cis* forms occurs almost completely. The back-photoisomerization to *cis* is achieved by heating. Using a dye-doped system, the lasing wavelength was tuned over 100 nm by controlling the UV irradiation time.

1.4.4 Mechanical Tuning

CLCs are noncompressive media, so compression does not affect the helical pitch. For CLC films, however, mechanical strain to CLC films with the helical axis along the film normal can induce the variation in pitch. Experiments have been performed using CLC elastomers [58]. Since the directors at surfaces are fixed, the helical pitch linearly changes with the compression rate. Using dye-doped CLC elastomers, red, green, and blue lasing emission was observed. The experiments were performed using biaxial strain, so uniform thickness change and associated uniform helix compression were achieved. If uniaxial strain is exerted, we obtain a deformed helix with shorter pitches. Since the refractive index change is not sinusoidal, it would be possible to observe higher order reflection. The experiment has not been performed so far.

1.4.5 Spatial Tuning

As mentioned above, a variety of external stimuli have been employed to control the helical pitch of CLCs. However, tunability is generally restricted within a narrow wavelength range at most 100 nm, and none of them supply tunability over the whole visible range. Chanishvili et al. [59, 60] and Huang et al. [61, 62] fabricated CLC structures with a spatial helical pitch gradient and tried to achieve lasing over a wide wavelength range. The former group used spatial gradient of chiral molecules, whereas the latter group used temperature gradient along the cell surface. Finally, Chanishvili et al. succeeded in obtaining position-dependent lasing emission over the whole visible range. Unfortunately, however, there was a window, where lasing was not possible [60]. Moreover, six or more kinds of dyes were necessary for wide-band lasing. On the other hand, Huang et al. [61] introduced temperature gradient across the cell and used temperature-dependent chiral dopant solubility to obtain the spatial-dependent pitch. Since they used reactive monomers as a host and polymerized, the pitch gradient was stable. However, the tuning range was only 50 nm because of the use of single dye. Later, they succeeded in expanding the tunable range to about 100 nm [62].

Narrow tunable range partly originates from emission bandwidth of the dye used. Actually, Chanishvili et al. [60] achieved a wide tunable range by using six or more dyes. Sonoyama et al. [63] used two dyes, coumarin and DCM, and succeeded in obtaining a wide tunable range covering the whole visible range without a wavelength window showing no lasing. Important points are summarized in Figure 1.16: (1) introduction of pitch gradient by temperature gradient, (2) introduction of concentration gradient of two dyes, and (3) energy transfer between two dyes. The emission band of coumarin dyes largely overlaps with the absorption band of DCM dyes, so efficient energy transfer is expected. Pumping light is absorbed by coumarin. The gradients in both pitch and dye concentration are important; at the shorter pitch region, emission of coumarin covers this region, so the region must be rich in coumarin. In the longer pitch region, on the contrary, the wavelength corresponds to the emission of DCM. Hence, this region must be rich in DCM. But at the same time, a certain amount of coumarin is also necessary to absorb pumping light. Finally, they succeeded in obtaining lasing emission covering the whole visible range from 470 to 670 nm by translating the cell with respect to a pumping beam, as shown in Figure 1.17 [63].

Another important effort was to make the lasing device temporally stable. Manabe et al. [64] used photopolymerizable CLCs and fixed the position-dependent pitch and dye concentration gradients by UV irradiation. Although the pitch slightly blue shifted by polymerization, position-dependent lasing over a full visible range was preserved. Photopolymerized CLC lasers with a helical axis lying within a substrate and with a pitch gradient were also fabricated [44]. In this case, the pitch gradient was

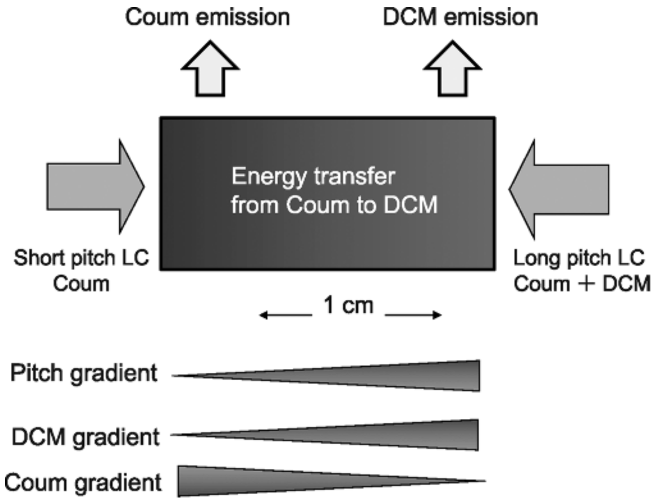

FIGURE 1.16 Gradients of pitch and dye concentration in a CLC cell for spatial lasing wavelength tuning.

realized by applying an electric field across wedged cells. These works opened the door of opportunity for a practical application as disposable dye lasers of a film form.

1.4.6 Multimode Lasing

We sometimes observed multiple lasing in (1) defect mode lasing from a thick defect layer [65], (2) simultaneous lasing of edge mode and defect mode [28], and (3) simultaneous lasing at both edges of PBG in single dye system [15] and (4) a Förster couple system [40]. However, the wavelength range of multiple lasing emission is limited within a very narrow range. Recently, Wang and Lin [66] obtained simultaneous nine lasing peaks around a 600–675 nm range. They prepared CLCs doped with chiral dopant exceeding the dissolving limit. As temperature increases, solubility increases and the helical pitch becomes shorter. The special uniformity of the dissolved chiral dopant depends upon the sample heating and cooling rates; that is, by increasing the cooling rate, the number of defects and domains increases, causing a multiple lasing.

To achieve wide-range simultaneous multiwavelength lasing such as red (R), green (G), and blue (B), a much sophisticated method to form wide-range multiple reflection bands is demanded. Ha et al. succeeded in obtaining RGB multiple reflection bands using multilayered structures of single-pitch CLC layers together with Fibonaccian defect [67] or isotropic defect layers [68], and then in RGB simultaneous lasing [69]. In order to explain the phenomenon, one of the key facts in CLC selective reflection is the cell thickness-dependent PBG width; the PBG width becomes broader and the reflectance decreases with decreasing sample thickness, as shown in Figure 1.17. Actually CLC with one-pitch ($1P$) thickness displays low

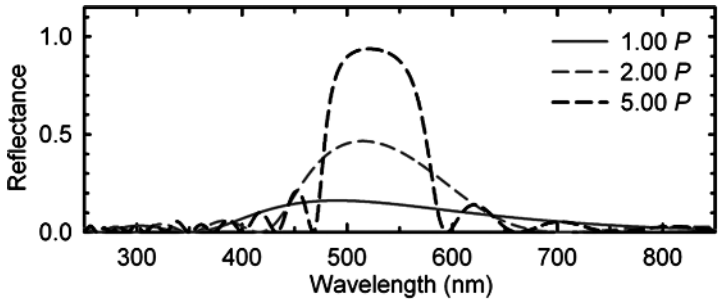

FIGURE 1.17 Selective reflection spectra in CLC cells with different thicknesses, 1, 2, and 5 pitch thick [78].

reflectance of 16% but the reflection band extends from 350 to 850 nm. If we insert isotropic defect layers, several reflection bands due to the defect mode may emerge within the wide PBG region. High reflectance can be achieved by increasing the number of CLC layers and defect layers alternately assembled. This is the fundamental idea of RGB or white light reflector [68].

They used PVA as a defect layer and constructed structures M_n = CLC/PVA/CLC/· · ·/CLC/PVA/CLC, where n stands for the number of CLC layers, as shown in Figure 1.18a. In Figure 1.18b are shown simulated (lower) and experimental (upper) reflection spectra for M_1, M_2, M_3, and M_4 systems [68]. These reflection spectra clearly indicate the presence of multiple PBGs from the multi-CLC systems. The agreement between experimental and calculated spectra is satisfactory. The physical parameters such as CLC and PVA film thicknesses obtained by theoretical fittings using the Berreman 4×4 matrix agreed with those experimentally obtained [68].

By using a dye-doped NLC sandwiched by M_4 layers with PCLC (1.5P/0.56 μm thick), simultaneous RGB lasing was achieved [69]. The same dye system as in Ref. 63 was used: coumarin and DCM. The excitation wavelength was 420 nm corresponding to the absorption peak of coumarin. As shown in Figure 1.19, the increase of

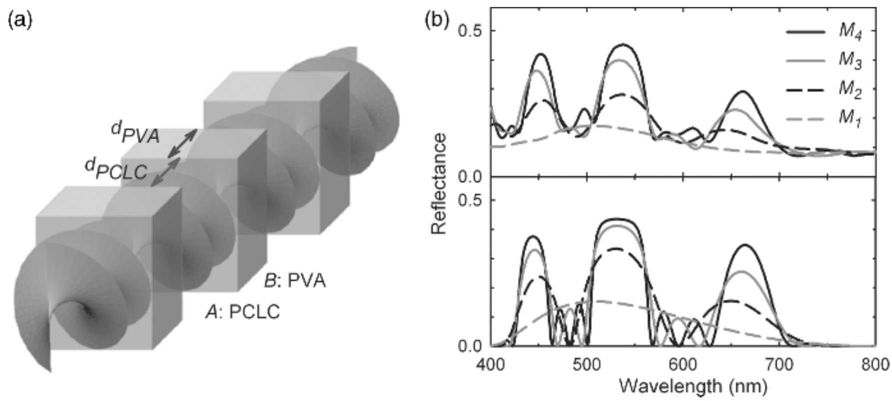

FIGURE 1.18 (a) Multistacked structures of CLC and PVA layers. (b) Experimental (upper) and simulated (lower) reflection spectra in four different multilayered cells [78].

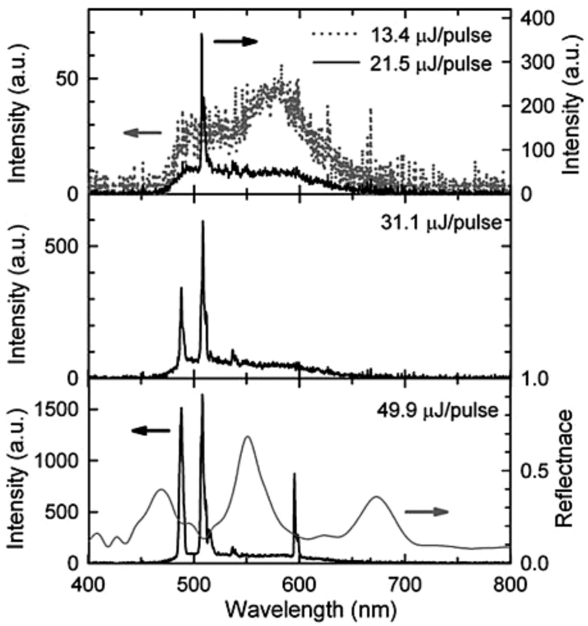

FIGURE 1.19 Multiple lasing emission spectra under different excitation powers. A reflection spectrum is also shown [78].

the pumping energy results in lasing at 508 nm (greenish, G) and 488 nm (bluish, B), and finally simultaneous RGB lasing emissions including 595 nm (reddish, R) light. This is unique as simultaneous RGB lasing occurs in a single resonator using single-pitched CLC with a single gain medium by a single optical pumping. Furthermore, each emission color of such lasings could be controlled by adjusting mixing ratios of two fluorescence dyes in the gain medium and optical pumping energies.

1.5 3D LC LASERS

Every LC laser mentioned so far has 1D cavity. One of the 3D structures whose periodicity could be in the visible range is obtained in the blue phase (BP). The first lasing using a dye-doped BP was reported by Cao et al. [70]. They actually observed different lasing peaks from three directions. Despite relatively low lasing threshold, the problem of using BP is always the temperature range of the phase. This problem was solved by Kikuchi et al. [71] by polymer stabilization. Using this technique, BP temperature range becomes 60 K including room temperature, although BP temperature range is usually only 1 K or so. Using such polymer-stabilized BP, lasing action was confirmed over 40 K [72].

Two types of 3D LC resonators have been reported by Humar et al. [73]. Both utilize liquid crystal droplets suspended in polymer matrices such as polydimethylsiloxane. Polymer dispersions of NLC droplets have been studied extensively in the

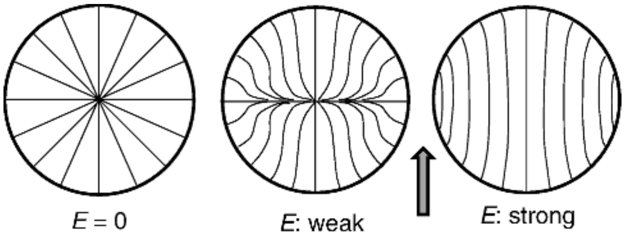

FIGURE 1.20 Director map of a NLC microdroplet embedded in polymer solution: (a) in the absence of an electric field, (b) under a weak electric field, and (c) under a strong electric field.

past, but individual droplets have never been considered as tunable optical resonators. The first one is a microresonator of dye-doped NLC droplets of about 10 μm diameter [73]. The microscope observation under crossed polarizers certifies the radial orientation of the NLC director, as shown in Figure 1.20a. When the NLC droplet was illuminated at the edge by a focused laser beam, a bright spot was observed at the other edge. In between, a light ring along the circumference of the microcavity was clearly visible. These observations clearly indicate whispering gallery modes (WGMs). Actually, they succeeded in observing spectra of WGMs circulating in a LC droplet. From the line width (about 0.055 nm), Q factor of the order of 12,000 was obtained. Lasing has not been reported using WGMs of this droplet. However, lasing capability using WGMs is well known in other systems [74], so lasing in LC WGMs is surely possible. Moreover, by deforming the sphere slightly, highly unidirectional lasing action would be possible [75], while lasing emission of WGMs of perfect sphere always emits tangentially. Another important aspect of the WGMs from LC microdroplets is tunability. By applying an electric field, director orientation in the droplet changes as shown in Figure 1.20b and c. Linear and reversible electrical tuning was obtained, and the tuning range could be over 40 nm by choosing proper LC materials.

The second type of 3D LC resonator was formed by using CLC droplet [76]. By using glycerol, the director is parallel to the interface of the droplet. Then, the formation of 3D helical structure with radial helical axes could be imagined (Figure 1.21). Lasing condition is the same as that in 1D DFB CLC lasers. Although the size of microdroplets cannot be controlled, lasing wavelength is uniquely defined by the helical pitch. An important point is that only dyes located at the center of droplets contribute to the lasing action (Figure 1.21), because the light emitted at the center is confined three dimensionally due to the radial helical axes; omnidirectional lasing emission occurs toward all the radial directions. Temperature-dependent helical pitch can also be used for tuning the laser light wavelength as in 1D DFB CLC lasers. A number of applications of the cholesteric onion microlasers were suggested by the authors [76]. One of the questions that still remained is polarization of laser light. The lasing emission is neither linearly nor circularly polarized. This could be due to the existence of many defects like in BP. Moreover, surface boundary condition of planar alignment does not define director orientation on the spherical surface. This is one of the future problems.

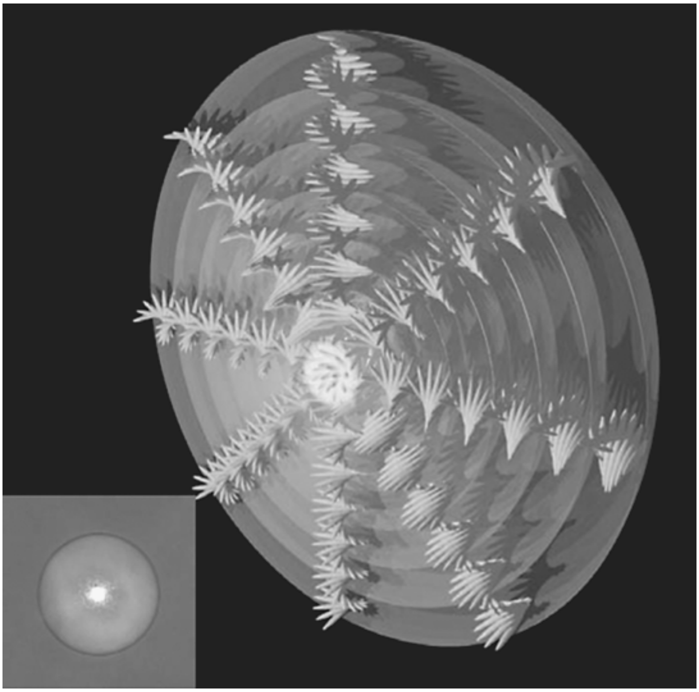

FIGURE 1.21 Helical structure in a CLC microdroplet. Image of microdroplet in a lasing condition is also shown [76]. (*See the color version of this figure in Color Plates section.*)

1.6 CONCLUSIONS

It has been more than three decades since the first observation of CLC laser emission in 1980 [10]. This field has been expanding rapidly particularly since Kopp et al. published a paper [11]. In this chapter, I focused on the most typical LC lasers, CLC microlasers. First, I described two kinds of CLC microlasers, DFB and defect mode lasers. Next, extensive efforts to lower the lasing threshold were summarized. They are classified into three kinds of improvements, that is, cavity structures, excitation conditions, and materials. Then, methods for tuning lasing wavelength, which is the most important feature of CLC lasers, were described. We can use variations in temperature, electric field, and light irradiation. Mechanical strain for polymer samples, spatial tuning for wide wavelength tuning, and multiple lasing over a wide wavelength range were also described. The readers may also refer recent review article [77]. Tunability is not only for wavelength, but also possible for polarization and directions, which I did not included in this chapter. Please refer to Ref. 78 for these tunabilities. 3D lasing is the most recent topic and provides us with promising devices. Much more application areas can be expected in 3D lasers such as telecommunications, optical computing, imaging devices, apparel and decoration, sensors, and biological imaging [76].

REFERENCES

1. E. Yablonovitch. Inhibited spontaneous emission in solid-state physics and electronics. *Phys. Rev. Lett.* **1987**, *58*, 2059–2062.
2. S. John. Strong localization of photons in certain disordered dielectric superlattices. *Phys. Rev. Lett.* **1987**, *58*, 2486–2489.
3. H. L. De Vries. Rotatory power and other optical properties of certain liquid crystals. *Acta Crystallogr.* **1951**, *4*, 219–226.
4. H. Takezoe, K. Hashimoto, Y. Ouchi, M. Hara, A. Fukuda, and E. Kuze. Experimental study on higher order reflection by monodomain cholesteric liquid crystals. *Mol. Cryst. Liq. Cryst.* **1983**, *101*, 329–340.
5. H. Takezoe, Y. Ouchi, M. Hara, A. Fukuda, and E. Kuze. Experimental studies on reflection spectra in monodomain cholesteric liquid crystal cells: total reflection, subsidiary oscillation and its beat or swell structure. *Jpn. J. Appl. Phys.* **1983**, *22*, 1080–1091.
6. D. W. Berreman. Optics in stratified and anisotropic media: 4×4 matrix formulation. *J. Opt. Soc. Am.* **1972**, *62*, 502–510.
7. H. Kogelnik and C. V. Shank. Coupled-wave theory of distributed feedback lasers. *J. Appl. Phys.* **1972**, *43*, 2327–2335.
8. R. Dreher and H. Schomburg. Prolongation of fluorescence decay time by structural changes of environment of emitting molecule. *Chem. Phys. Lett.* **1974**, *25*, 527–530.
9. M. Hara, H. Takezoe, A. Fukuda, E. Kuze, Y. Kaizu, and H. Kobayashi. Influence of cholesteric Bragg reflection of spontaneous emission from the inside of the helical structure. *Mol. Cryst. Liq. Cryst.* **1985**, *116*, 253–263.
10. I. P. Il'chishin, E. A. Tikhonov, V. G. Tishchenko, and M. T. Shpak. Generation of a tunable radiation by impurity cholesteric liquid crystals. *JETP Lett.* **1980**, *32*, 24–27.
11. V. I. Kopp, F. Fan, H. K. M. Vitana, and A. Z. Genack. Low-threshold lasing at the edge of a photonic stop band in cholesteric liquid crystals. *Opt. Lett.* **1998**, *23*, 1707–1709.
12. R. Bartolino and L. M. Blinov. Liquid crystal microlasers (introductory notes) In: L. M. Blinov and R. Bartolino, Eds., *Liquid Crystal Microlasers*, Transworld Research Network, Kerala, 2010, Chapter 1.
13. V. I. Kopp, Z.-Q. Zhang, and A. Z. Genack. Lasing in chiral photonic structures. *Prog. Quant. Electron.* **2003**, *27*, 369–416.
14. J. P. Dowling, M. Scalora, M. J. Bloemer, and C. M. Bowden. The photonic band edge laser: a new approach to gain enhancement. *J. Appl. Phys.* **1994**, *74*, 1896–1899.
15. K.-C. Shin, F. Araoka, B. Park, Y. Takanishi, K. Ishikawa, Z. Zhu, T. M. Swager, and H. Takezoe. Advantages of highly ordered polymer-dyes for lasing in chiral nematic liquid crystals. *Jpn. J. Appl. Phys.* **2004**, *43*, 631–636.
16. J. Schmidtke and W. Stille. Fluorescence of a dye-doped cholesteric liquid crystal film in the region of the stop band: theory and experiment. *Eur. Phys. J. B* **2003**, *31*, 179–194.
17. E. Yablonovitch, T. J. Gmitter, R. D. Meade, A. M. Rappe, K. K. Brommer, and J. D. Joannopoulos. Donor and acceptor modes in photonic band structure. *Phys. Rev. Lett.* **1991**, *67*, 3380–3383.
18. R. Ozaki, T. Matsui, M. Ozaki, and K. Yoshino. Electrically color-tunable defect mode lasing in one-dimensional photonic-band-gap system containing liquid crystal. *Appl. Phys. Lett.* **2003**, *82*, 3593-1–3593-3.

19. O. Painter, P. K. Lee, A. Scherer, A. Yariv, J. D. O'Brien, P. D. Dapkus, and I. Kim. Two-dimensional photonic band-gap defect mode laser. *Science* **1999**, *284*, 1819–1821.
20. S. G. Johnson and J. C. Joannopoulos. Three-dimensionally periodic dielectric layered structure with omnidirectional photonic band gap. *Appl. Phys. Lett.* **2000**, *77*, 3490-1–3490-3.
21. K. M. Ho, C. T. Chan, and C. M. Soukoulis. Existence of a photonic gap in periodic dielectric structures. *Phys. Rev. Lett.* **1990**, *65*, 3152–3155.
22. V. I. Kopp and A. Z. Genack. Twist defect in chiral photonic structures. *Phys. Rev. Lett.* **2002**, *89*, 033901-1–033901-4.
23. J. Schmidtke, W. Stille, and H. Finkelmann. Defect mode emission of a dye doped cholesteric polymer network. *Phys. Rev. Lett.* **2003**, *90*, 083902-1–083902-4.
24. M. Ozaki, R. Ozaki, T. Matsui, and K. Yoshino. Twist-defect-mode lasing in photopolymerized cholesteric liquid crystal. *Jpn. J. Appl. Phys.* **2003**, *42*, L472–L475.
25. H. Hoshi, K. Ishikawa, and H. Takezoe. Optical second-harmonic generation enhanced by a twist defect in ferroelectric liquid crystals. *Phys. Rev. E* **2003**, *68*, 020701(R)-1–020701 (R)-3.
26. Y.-C. Yang, C.-S. Kee, J.-E. Kim, and H. Y. Park. Photonic defect modes of cholesteric liquid crystals. *Phys. Rev. E* **1999**, *60*, 6852–6854.
27. S. M. Jeong, N. Y. Ha, Y. Takanishi, K. Ishikawa, and H. Takezoe. Defect mode lasing from a double-layered dye-doped polymeric cholesteric liquid crystal films with a thin rubbed defect layer. *Appl. Phys. Lett.* **2007**, *90*, 261108-1–261108-3.
28. M. H. Song, B. Park, K.-C. Shin, T. Ohta, Y. Tsunoda, H. Hoshi, Y. Takanishi, K. Ishikawa, J. Watanabe, S. Nishimura, T. Toyooka, Z. Zhu, T. M. Swager, and H. Takezoe. Effect of phase retardation on defect-mode lasing in polymeric cholesteric liquid crystals. *Adv. Mater.* **2004**, *16*, 779–783.
29. M. H. Song, N. Y. Ha, K. Amemiya, B. Park, Y. Takanishi, K. Ishikawa, J. W. Wu, and H. Takezoe. Defect-mode lasing with lowered threshold in a three-layered heterocholesteric liquid-crystal structure. *Adv. Mater.* **2006**, *18*, 193–197.
30. J. Schmidtke and W. Stille. Photonic defect modes in cholesteric liquid crystal films. *Eur. Phys. J. E* **2003**, *12*, 553–564.
31. T. Matsui, M. Ozaki, and K. Yoshino. Tunable photonic defect modes in a cholesteric liquid crystal induced by optical deformation of helix. *Phys. Rev. E* **2004**, *69*, 061715-1–061715-4.
32. K. Amemiya, T. Nagata, M. H. Song, Y. Takanishi, K. Ishikawa, S. Nishimura, T. Toyooka, and H. Takezoe. Enhancement of laser emission intensity in dye-doped liquid crystals with single-output window. *Jpn. J. Appl. Phys.* **2005**, *44*, 3748–3750.
33. Y. Matsuhisa, R. Ozaki, Y. Takao, and M. Ozaki. Linearly polarized lasing in one-dimensional hybrid photonic crystal containing cholesteric liquid crystal. *J. Appl. Phys.* **2007**, *101*, 033120-1–033120-4.
34. V. A. Belyakov. Low threshold DFB lasing in chiral LC at diffraction of pumping wave. *Mol. Cryst. Liq. Cryst.* **2006**, *435*, 43–69.
35. Y. Matsuhisa, Y. Huang, Y. Zhou, and S.-T. Wu. Low-threshold and high efficiency lasing upon band-edge excitation in a cholesteric liquid crystal. *Appl. Phys. Lett.* **2007**, *90*, 091114-1–091114-3.

36. Y. Wang, T. Manabe, Y. Takanishi, K. Ishikawa, G. Shao, A. Orita. J. Otera, and H. Takezoe. Dependence of lasing threshold power on excitation wavelength in dye-doped cholesteric liquid crystals. *Opt. Commun.* **2007**, *280*, 408–411.
37. M. G. Chee, M. H. Song, D. Kim, H. Takezoe, and L. J. Chung. Lowering lasing threshold in chiral nematic liquid crystal structure with different anisotropies. *Jpn. J. Appl. Phys.* **2007**, *46*, L437–L439.
38. F. Araoka, K.-C. Shin, Y. Takanishi, K. Ishikawa, H. Takezoe, Z. Zhu, and T. M. Swager. How doping a cholesteric liquid crystal with polymeric dye improves an order parameter and makes possible low threshold lasing. *J. Appl. Phys.* **2003**, *94*, 279–283.
39. K. Sonoyama, Y. Takanishi, K. Ishikawa, and H. Takezoe. Lowering threshold by energy transfer between two dyes in cholesteric liquid crystal distributed feedback lasers. *Appl. Phys. Exp.* **2008**, *1*, 032002-1–032002-3.
40. M. Chambers, M. Fox, M. Grell, and J. Hill. Lasing from a Forster transfer fluorescent dye couple dissolved in a chiral nematic liquid crystals. *Adv. Funct. Mater.* **2002**, *12*, 808–810.
41. M. Uchimura, Y. Watanabe, F. Araoka, J. Watanabe, H. Takezoe, and G. Konishi. Development of laser dyes to realize low threshold in dye-doped cholesteric liquid crystal lasers. *Adv. Mater.* **2010**, *22*, 4473–4478.
42. S. K. H. Wei, S. H. Chen, K. Dolgaleva, S. G. Lukishova, and R. W. Boyd. Robust organic lasers comprising glassy-cholesteric pentafluorene doped with a red-emitting oligofluorene. *Appl. Phys. Lett.* **2009**, *94*, 041111-1–041111-3.
43. K. Funamoto, M. Ozaki, and K. Yoshino. Discontinuous shift of lasing wavelength with temperature in cholesteric liquid crystal. *Jpn. J. Appl. Phys.* **2003**, *42*, L1523–L1525.
44. H. Yoshida, Y. Inoue, T. Isomura, Y. Matsuhisa, A. Fujii, and M. Ozaki. Position sensitive, continuous wavelength unable laser based on photopolymerizable cholesteric liquid crystals with an in-plane helix alignment. *Appl. Phys. Lett.* **2009**, *94*, 093306-1–093306-3.
45. G. Strangi, V. Barna, R. Caputo, A. de Luca, C. Versace, N. Scaramuzza, C. Umeton, and R. Bartolino. Color-tunable organic microcavity laser array using distributed feedback. *Phys. Rev. Lett.* **2005**, *94*, 063903-1–063903-4.
46. M. Kasano, M. Ozaki, and K. Yoshino. Electrically tunable waveguide laser based on ferroelectric liquid crystal. *Appl. Phys. Lett.* **2003**, *82*, 4026–4028.
47. S. M. Morris, A. D. Ford, and H. J. Coles. Removing the discontinuous shifts in emission wavelength of a chiral nematic liquid crystal laser. *J. Appl. Phys.* **2009**, *106*, 023112-1–023112-4.
48. Y. Huang, Y. Zhou, C. Doyle, and S.-T. Wu. Tuning the photonic band gap in cholesteric liquid crystals by temperature-dependent dopant solubility. *Opt. Express* **2006**, *14*, 1236–1242.
49. M. Ozaki, M. Kasano, T. Kitasho, D. Ganzke, W. Hasse, and K. Yoshino. Electro-tunable liquid-crystal lasers. *Adv. Mater.* **2003**, *15*, 974–977.
50. M. H. Song, B. Park, S. Nishimura, T. Toyooka, I. J. Chung, Y. Takanishi, K. Ishikawa, and H. Takezoe. Electrotunable non-reciprocal laser emission from a liquid-crystal photonic device. *Adv. Funct. Mater.* **2006**, *16*, 1793–1798.
51. M. H. Song, B. Park, K.-C. Shin, T. Ohta, Y. Tsunoda, H. Hoshi, Y. Takanishi, K. Ishikawa, J. Watanabe, S. Nishimura, T. Toyooka, Z. Zhu, T. M. Swager, and H. Takezoe. Lasing characteristics of a dye-doped nematic liquid crystal layer sandwiched by two polymeric cholesteric liquid crystals. *Proc. SPIE* **2004**, *5518*, 66–76.

52. T.-H. Lin, H.-C. Jau, C.-H. Chen, Y.-J. Chen, T.-H. Wei, C.-W. Chen, and A. Y.-G. Fuh. Electrically controllable laser based on cholesteric liquid crystal with negative dielectric anisotropy. *Appl. Phys. Lett.* **2006**, *88*, 061122-1–061122-3.
53. B. Park, M. Kim, S. W. Kim, W. Jang, H. Takezoe, Y. Kim, E. H. Choi, Y. H. Seo, G. S. Cho, and S. O. Kang. Electrically controllable omnidirectional laser emission from a helical-polymer network composite film. *Adv. Mater.* **2009**, *21*, 771–775.
54. W. Helfrich. Electrohydrodynamic and dielectric instabilities of cholesteric liquid crystals. *J. Chem. Phys.* **1971**, *55*, 839–842.
55. A. Chanishvili, G. Chilaya, and G. Petriashvili. Phototunable lasing in dye-doped cholesteric liquid crystals. *Appl. Phys. Lett.* **2003**, *83*, 5353–5355.
56. S. Furumi, S. Yokoyama, A. Otomo, and S. Mashiko. Phototunable photonic bandgap in a chiral liquid crystal laser device. *Appl. Phys. Lett.* **2004**, *84*, 2491–2493.
57. T.-H. Lin, Y.-J. Chen, C.-H. Wu, A. Y.-G. Fuh, J.-H. Liu, and P.-C. Yang. Cholesteric liquid crystal laser with wide tuning capability. *Appl. Phys. Lett.* **2005**, *86*, 161120-1–161120-3.
58. H. Finkelmann, S. T. Kim, A. Munoz, P. Palffy-Muhoray, and B. Taheri. Tunable mirrorless lasing in cholesteric liquid crystalline elastomers. *Adv. Mater.* **2001**, *13*, 1069–1072.
59. A. Chanishvili, G. Chilaya, G. Petriashvili, R. Barberi, R. Bartolino, G. Cipparrone, A. Mazzulla, and L. Oriol. Lasing in dye-doped cholesteric liquid crystals: two new tuning strategies. *Adv. Mater.* **2004**, *16*, 791–795.
60. A. Chanishvili, G. Chilaya, G. Petriashvili, R. Barberi, R. Bartolino, G. Cipparrone, A. Mazzulla, R. Gimenex, L. Oriol, and M. Pinol. Widely tunable ultraviolet–visible liquid crystal laser. *Appl. Phys. Lett.* **2005**, *86*, 051107-1–051107-3.
61. Y. Huang, L.-P. Chen, C. Doyle, Y. Zhou, and S.-T. Wu. Spatially tunable laser emission in dye-doped cholesteric polymer films. *Appl. Phys. Lett.* **2006**, *89*, 111106-1–111106- 3.
62. Y. Huang, Y. Zhou, and S.-T. Wu. Spatially tunable laser emission in dye-doped photonic liquid crystals. *Appl. Phys. Lett.* **2006**, *88*, 111107-1–111107-3.
63. K. Sonoyama, Y. Takanishi, K. Ishikawa, and H. Takezoe. Position-sensitive cholesteric liquid crystal dye laser covering a full visible range. *Jpn. J. Appl. Phys.* **2007**, *46*, L874–L876.
64. T. Manabe, K. Sonoyama, Y. Takanishi, K. Ishikawa, and H. Takezoe. Toward practical application of cholesteric liquid crystals to tunable lasers. *J. Mater. Chem.* **2008**, *18*, 3040–3043.
65. M. H. Song, B. Park, Y. Takanishi, K. Ishikawa, S. Nishimura, T. Toyooka, and H. Takezoe. Lasing from thick anisotropic layer sandwiched between polymeric cholesteric liquid crystal films. *Jpn. J. Appl. Phys.* **2005**, *44*, 8165–8167.
66. C.-T. Wang and T.-H. Lin. Multi-wavelength laser emission in dye-doped photonic liquid crystals. *Opt. Express* **2008**, *16*, 18334–18339.
67. N. Y. Ha, Y. Takanishi, K. Ishikawa, and H. Takezoe. Simultaneous RGB reflections from single-pitched cholesteric liquid crystal films with Fibonaccian defects. *Opt. Express* **2007**, *15*, 1024–1029.
68. N. Y. Ha, Y. Ohtsuka, S. M. Jeong, S. Nishimura, G. Suzaki, Y. Takanishi, K. Ishikawa, and H. Takezoe. Fabrication of a simultaneous red–green–blue reflector using single-pitched cholesteric liquid crystals. *Nat. Mater.* **2008**, *7*, 43–47.

69. N. Y. Ha, S. M. Jeong, S. Nishimura, G. Suzaki, K. Ishikawa, and H. Takezoe. Simultaneous red, green, blue lasing emission in a single-pitched cholesteric liquid-crystal system. *Adv. Mater.* **2008**, *20*, 2503–2507.
70. W. Cao, A. Munoz, P. Palffy-Muhoray, and B. Taheri. Lasing in a three-dimensional photonic crystal of the liquid crystal blue phase II. *Nat. Mater.* **2002**, *1*, 111–113.
71. H. Kikuchi, M. Yokota, Y. Hisakado, H. Yang, and T. Kajiyama. Polymer-stabilized liquid crystal blue phases. *Nat. Mater.* **2002**, *1*, 64–68.
72. S. Yokoyama, S. Mashiko, H. Kikuchi, K. Uchida, and T. Nagamura. Laser emission from a polymer-stabilized liquid-crystalline blue phase. *Adv. Mater.* **2006**, *18*, 48–51.
73. M. Humar, M. Ravnik, S. Pajk, and I. Musevic. Electrically tunable liquid crystal optical microresonators. *Nat. Photon.* **2009**, *3*, 595–600.
74. V. Snadoghdar, F. Treussart, J. Hare, V. Lefevre-Seguin, J.-M. Raimond, and S. Haroche. Very low threshold whispering-gallery-mode microsphere laser. *Phys. Rev. A.* **1996**, *54*, R1777–R1780.
75. Q. J. Wang, C. Yan, N. Yu, J. Unterhinninghofen, J. Wiersig, C. Pflugl, L. Diehl, T. Edamura, M. Yamanishi, H. Kan, and F. Capasso. Whispering-gallery mode resonators for highly unidirectional laser action. *Proc. Natl. Acad. Sci. USA* **2010**, *107*, 22407–22412.
76. M. Humar and I. Musevic. 3D microlasers from self-assembled cholesteric liquid-crystal microdroplets. *Opt. Express* **2010**, *18*, 26995–27003.
77. H. Coles and S. Morris. Liquid-crystal lasers. *Nat. Photon.* **2010**, *4*, 676–685.
78. H. Takezoe, N. Y. Ha, M. H. Song, S. M. Jeong, and B. Park. Tuning laser light from liquid crystal lasers. In: L. M. Blinov and R. Bartolino, Eds., *Liquid Crystal Microlasers*, Transworld Research Network, Kerala, 2010, Chapter 4.
79. H. Takezoe. Photonic devices using liquid crystal; nanostructures. In: H. Hosono, Y. Mishima, H. Takezoe, K.J.D. Mackenzie, Eds., *Nanomaterials -from research to applications-*, Elsevier, London, 2006, Chapter 4.